

# Fabrication of nanocrystalline nickel coatings by brush plating

T. Shang<sup>1</sup>, H. Z. Zhang<sup>2</sup>, H. Jiang<sup>2</sup>, L. Dai<sup>3</sup>, G. L. Zhang<sup>4</sup> and X. L. Liu<sup>\*4</sup>

Nanocrystalline nickel coatings were fabricated on smooth steel substrates using electric brush plating technology. The coatings were characterised by X-ray diffraction, scanning electron microscopy, field emission scanning electron microscopy and atomic force microscope. Cetyltrimethyl ammonium bromide (CTAB) as cationic surfactant is used to improve the surface morphologies of coatings. With the content of CTAB increasing in electrolyte, the size of microscale nodules consisting of nanoscale grains were reduced, (111) texture was formed, and the surface having totally single nanosized grains structure was prepared on the surface of brush plating coatings. The formation mechanisms of nickel coatings deposited were also analysed based on the process of deoxidisation, adsorbing and withdrawing.

**Keywords:** Brush plating, Nanocrystalline, Nickel coating, CTAB

## Introduction

Nanocrystalline materials have exhibited many unusual mechanical, physical and electrochemical properties compared with their conventional polycrystalline counterparts.<sup>1–5</sup> The search for nanocrystalline metallic coatings has received a considerable attention during the past decades due to their existing or potential applications.<sup>3,4</sup> The results show that grain size, surface morphology and texture of nanocrystalline coatings can improve their properties, for example the wear and corrosion resistance.<sup>2,3</sup> Electrodeposition has been recognised as the most technologically feasible and economically superior technique among all kinds of fabrication methods.<sup>1,4,5</sup>

Electric brush plating technology, as one of the methods of electrodeposition, has been applied widely to fabricate metallic and composite coatings in engineering.<sup>6–8</sup> The coatings can be deposited on the surfaces of arbitrary size and shape. The equipments are portability, flexibility and easy to operate. The cost of coatings deposited is lower than vapour deposition and sputter deposition. Many researches devoted to morphologies, microstructure, mechanical and chemical properties of brush plating coatings.<sup>9,10</sup> With grain size decreasing, the corrosion and tribological behaviour of nanocrystalline coating is improved.<sup>11–13</sup> The nanostructure and low surface roughness are helpful to obtain high water contact angle on the deposited surface.<sup>14</sup> The

aim of this paper is to fabricate the nanocrystalline nickel coating, research the effect of CTAB content added in the plating bath on surface morphology and analyse the deposition mechanism.

## Experimental

Nanocrystalline Nickel coatings were synthesised by brush plating using a sulphate based electrolyte. The steel plate (cathode) (C1008, AISI) was used as the substrate. The stylus (anode) with a carbon block was wrapped with cotton and polypropylene fabric with proper thickness. Polypropylene fabric has a certain rigidity and higher antiabrasion than other absorbent membrane. The stylus was connected with the positive electrode of the Power Pack MODEL DSD-75-9 and the substrate with negative. Before brush plating, the substrate surfaces were polished with 1200 and 1500 mesh sandpapers and abrasive and rinsed with ethanol followed by acetone. The brush plating was performed at room temperature (RT) with a deposition rate of  $\sim 12 \text{ m min}^{-1}$  and an electric voltage deposition of  $\sim 12 \text{ V}$ . The plating solution was recirculated continuously from the solution tank to the work area through a tube by means of a pump. The composition of a litre brush plating solution was 254 g  $\text{NiSO}_4 \cdot 7\text{H}_2\text{O}$ , 56 g  $(\text{NH}_4)_3\text{C}_6\text{H}_5\text{O}_7$ , 23 g  $\text{CH}_3\text{COONH}_4$ , 105 g  $\text{NH}_3 \cdot \text{H}_2\text{O}$  (25%).<sup>15</sup> As a cationic type surfactant, cetyltrimethyl ammonium bromide [ $\text{C}_{16}\text{H}_{33}(\text{CH}_3)_3\text{NBr}$ ] was added into above electrolyte to improve the surface morphologies of brush plating coatings under strong magnetic stirring. The thickness of coatings was ensured using the Coulometric method and the weight of sample was measured before and after brush plating.

Crystalline structure and grain size of coatings were characterized by the X-ray diffraction analysis (XRD, D/max-2500PC, Rigaku) using the standard reflection mode with  $\text{Cu K}_\alpha$  ( $\lambda = 0.154056 \text{ nm}$ ) in the region of

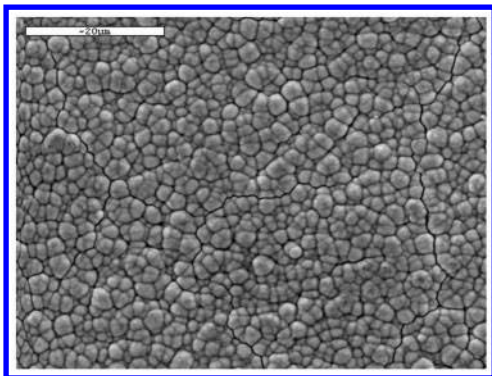
<sup>1</sup>College of Machine Science and Engineering, Jilin University, Nanling Campus, Changchun 130025, China

<sup>2</sup>Changchun Institute of Engineering Technology, Changchun 130117, China

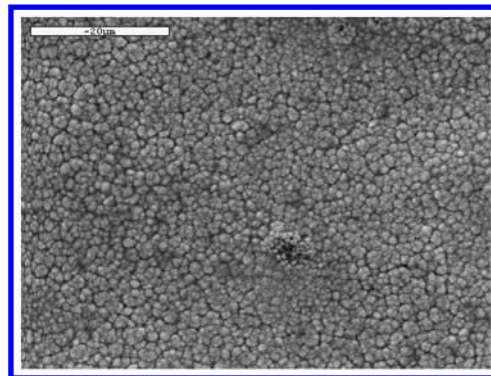
<sup>3</sup>Changchun Institute of Optics, Fine Mechanics and Physics, Chinese Academy of Sciences, Changchun 130033, China

<sup>4</sup>Key Laboratory of Bionic Engineering (Ministry of Education), Jilin University, Nanling Campus, Changchun 130025, China

\*Corresponding author, email lx5211@126.com



1 SEM surface morphology of coating deposited using non-containing CTAB plating solution

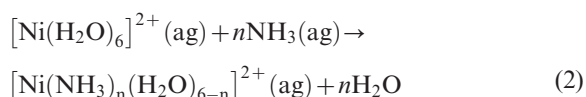
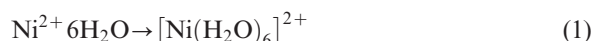


2 SEM surface morphology of coating deposited using containing 5 g L<sup>-1</sup> CTAB plating solution

$20^\circ < 2\theta < 80^\circ$  with the scanning rate and step being  $4^\circ \text{ min}^{-1}$  and  $0.02^\circ$  respectively. Surface morphologies were characterized by scanning electron microscopy (SEM, JSM-5600, JEOL, Japan), field emission scanning electron microscopy (FESEM, S-4300 Hitachi and JSM-6700F JEOL, Japan) equipped with an energy dispersive spectroscopy (EDS). Surface roughness was characterized by atomic force microscope (AFM, Nanoscope IIIa, Digital Instruments, USA) using the silicon cantilever for the tapping mode.

## Results and discussion

It is known that some metallic ions with  $\text{H}_2\text{O}$  can form hexa-aqua complexes of  $[\text{M}(\text{H}_2\text{O})_6]^{3+}$  ( $\text{M} = \text{Sc}^{3+}$  to  $\text{Fe}^{3+}$ ) and  $[\text{Me}(\text{H}_2\text{O})_6]^{2+}$  ( $\text{Me} = \text{Co}^{2+}$ ,  $\text{Ni}^{2+}$ ,  $\text{Cu}^{2+}$  and  $\text{Zn}^{2+}$ ).<sup>16</sup>  $[\text{Ni}(\text{H}_2\text{O})_6]^{2+}$  is predicted to be the most stable among all complexes of  $\text{Ni}^{2+}$  and  $\text{H}_2\text{O}$ .  $\text{H}_2\text{O}$  ligands in  $[\text{Ni}(\text{H}_2\text{O})_6]^{2+}$  can be replaced successively by  $\text{NH}_3$  ligands with higher polarisability to form six different complexes of coordinate  $[\text{Ni}(\text{NH}_3)_n(\text{H}_2\text{O})_{6-n}]^{2+}$  ( $n=0-6$ ) (equation (2)), which results in a monotonic increasing in the average metal-ligand bond length and the stabilization energy of the complexes.<sup>16</sup> The chemical reactions are likely to be described as follows



Basing on above results, complexes of  $\text{Ni}^{2+}$  in brush plating solution might be  $[\text{Ni}(\text{NH}_3)_n(\text{H}_2\text{O})_{6-n}]^{2+}$  ( $\text{pH} \approx 7.5$ ) transformed from  $[\text{Ni}(\text{H}_2\text{O})_6]^{2+}$  ( $\text{pH} \approx 2.0$ ). The discharge speed of  $[\text{Ni}(\text{NH}_3)_n(\text{H}_2\text{O})_{6-n}]^{2+}$  complexes is faster than  $[\text{Ni}(\text{H}_2\text{O})_6]^{2+}$  resulting in higher nucleation rate, because the bond energy is expected to vary inversely with bond length.<sup>16</sup> In the brush plating process,  $[\text{Ni}(\text{NH}_3)_n(\text{H}_2\text{O})_{6-n}]^{2+}$  obtains electrons and is reduced into metal nickel (equation (3))

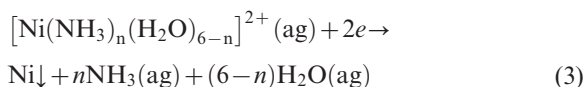
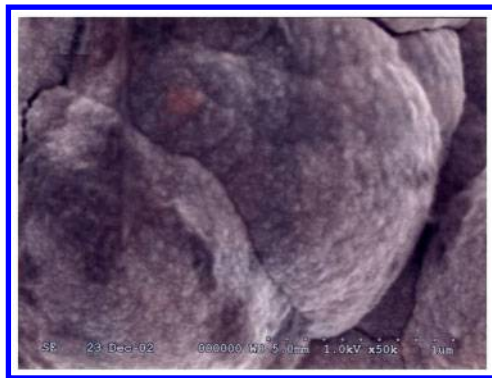


Figure 1 shows the SEM surface morphology of brush plating nickel coating (non- containing CTAB in the plating solution). It can be seen that the surface is composed of uniformly distributed small nodules units with an average size of  $2.5\text{--}3.5 \mu\text{m}$ , no pores are found

and a few microcracks observed. Such surface morphology consisting of micron-sized nodules is similar to the surface morphology observed on cauliflower.<sup>17</sup> This result may be attributed to the continuous supply of plating solution, appropriate contact pressure and movement speed between anode and cathode.

It is well known that microstructural characterisation of the coatings is important as it helps to better understand its macroscopic behaviour. CTAB as a cationic surfactant has been used to improve the surface morphologies on the coatings deposited in electrodeposition<sup>18</sup> and electroless.<sup>19</sup> For the plating solution with CTAB, CTAB molecule can be dissociated to cetyltrimethyl ammonium cation ( $\text{CTA}^+$ ,  $[\text{C}_{16}\text{H}_{33}\text{N}(\text{C}_3\text{H}_3)_3]^+$ ) and  $\text{Br}^-$  anion in aqueous solution.<sup>18</sup> Before brush plating, the substrate surface was covered with plating solution and  $\text{CTA}^+$  can be adsorbed rapidly on the substrate surface under the effect of electric field. Studies indicate only cationic surfactants are adsorbed on the cathode surface in the plating solution of  $[\text{C}_{16}\text{H}_{33}\text{N}(\text{C}_3\text{H}_3)_3]^+$  and  $[\text{Ni}(\text{NH}_3)_n(\text{H}_2\text{O})_{6-n}]^{2+}$  coexistence.<sup>20,21</sup> Owing to  $\text{CTA}^+$  adsorbed preferentially effect, the contact between  $[\text{Ni}(\text{NH}_3)_n(\text{H}_2\text{O})_{6-n}]^{2+}$  and substrate was baffled.<sup>21</sup> In the brush plating process, the stylus moves uniformly on the work surface and  $\text{CTA}^+$  can be withdrawn from the substrate surface by stylus and  $[\text{Ni}(\text{NH}_3)_n(\text{H}_2\text{O})_{6-n}]^{2+}$  can contact with cathode surface.  $[\text{Ni}(\text{NH}_3)_n(\text{H}_2\text{O})_{6-n}]^{2+}$  ions were reduced into metal nickel at the movable contact area between polypropylene fabric and cathode. At the non-contact area,  $\text{CTA}^+$  was adsorbed again on the brush plating surface and the reduction reaction of  $[\text{Ni}(\text{NH}_3)_n(\text{H}_2\text{O})_{6-n}]^{2+}$  ions did not be happened. Crystalline nickel can be deposited by the means of layer-layer with stylus moving to and fro.

Figure 2 shows the surface morphology of coating deposited using containing  $5 \text{ g L}^{-1}$  CTAB in the plating solution. It can be seen that the coating is similar to that observed in Fig. 1 and the size of nodules units is obviously decreased to  $1.2\text{--}1.5 \mu\text{m}$  (Fig. 2). The FESEM is used to make a clear observation because the fine grain size within nodules could not be resolved by conventional SEM observations. Figure 3 shows the micro-sized nodules are due to agglomeration of nanosized grains. The mean size of nodules is consistent with the SEM result (Fig. 2). The size of grains within nodules is about  $10\text{--}12 \text{ nm}$ . Such surface morphology consisting of micro-sized nodules that are composed of nanosized grains can be regarded as the micro- and nanoscale structure.

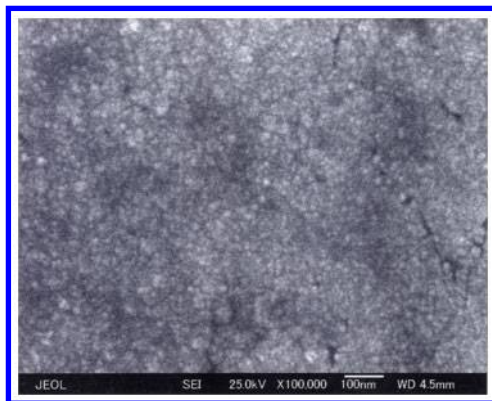


3 FESEM surface morphology of coating deposited using containing  $5 \text{ g L}^{-1}$  CTAB plating solution

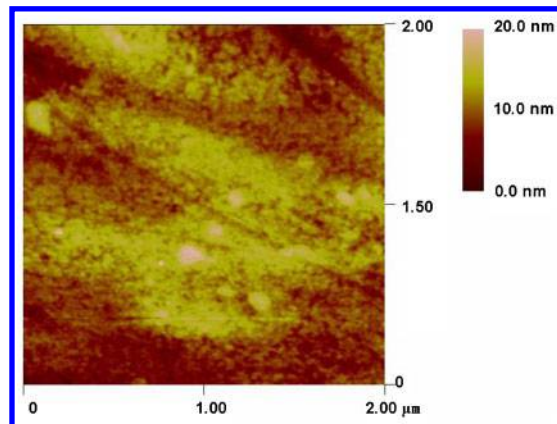
To surface morphology of the coating deposited using containing  $15 \text{ g L}^{-1}$  CTAB in the plating solution, the surface shows a quite uniform and compact nanosized grains structure observed from FESEM observation (Fig. 4). Nodules, agglomerates crystallite clusters, hollows, and vacancies were not detected. The size of grains is about 12–14 nm. Such morphology is primarily attributed to the effect of higher CTAB content in the plating solution except for the above reason. The as deposited surface of the nanosized grains coating exhibited a flat and mirror-like appearance, which hints that such surface has a lowest surface roughness. Figure 5 shows the surface roughness (Rms) determined by AFM (scan area is  $2 \times 2 \mu\text{m}$ ) is  $\sim 2.685 \text{ nm}$  corresponding Fig. 4.

Above results show the CTAB added in plating solution can prevent effectively agglomerate tendency of the nanosized nickel grains. With the CTAB content increasing, the size of nickel nodules is decreased. The nickel nodules can be extinct when the content of CTAB increases into an appropriate extent. The size of grains in nickel coatings increases from 10–12 to 12–14 nm with the CTAB content in the plating solution increasing from 5 to  $15 \text{ g L}^{-1}$ . Therefore, it is infinitesimal the effect of content of CTAB on the size of grains in nickel coatings.

X-ray diffraction patterns of the electric brush plating nickel coatings fabricated using the plating solution containing  $15 \text{ g L}^{-1}$  CTAB are shown in Fig. 6. It can be clearly seen that the typical diffraction peaks characteristic of polycrystalline nickel (JCPDS 04-0850) is observed and any other phases are not be detected. The



4 FESEM surface morphology of coating deposited using containing  $15 \text{ g L}^{-1}$  CTAB plating solution

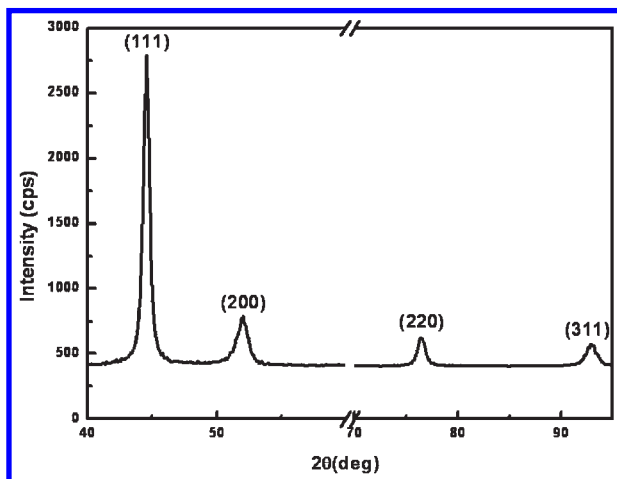


5 AFM surface morphology of coating deposited using containing  $15 \text{ g L}^{-1}$  CTAB plating solution

determination of the full width at half maximum (FWHM) of Bragg peaks can yield information on crystal sizes. The highest intensity plane of diffraction obtained from XRD has been used to evaluate the average grain sizes for nanocrystalline metals coatings. Hence, line broadening measurements of the electric brush plating coatings were performed using the 100% intensity (111) plane of diffraction to ascertain crystallite size using the classical Debye–Scherrer formula. Result shows that the mean grain size is  $\sim 12 \text{ nm}$ . The diffraction intensity ratio of the (111) to (200) peaks ( $I(111)/I(200)$ ) is  $\sim 2.083$  in a standard polycrystalline nickel diffraction pattern. The  $I(111)/I(200)$  is 3.590 in Fig. 6, which proved that the (111) texture can be formed in brush plating nickel coating. The mean size of grains determined by the X-ray diffraction is consistent with FESEM (Fig. 4).

## Conclusion

Nanocrystalline nickel coatings can be synthesised by brush plating technology and CTAB is added in the plating solution. With the content of CTAB increasing, the structure on the coating surface can be transformed into totally single nanosized grains with about 12–14 nm grains and 2.685 nm Rms from microscale nodules consisting of nanoscale grains, the size of nodules can be reduced effectively, and the (111) texture can be formed,



6 X-ray diffraction patterns of coatings deposited using containing  $15 \text{ g L}^{-1}$  CTAB plating solution

but the size of grains can be influenced hardly. The coatings can be fabricated by the way of deoxidisation, adsorbing and withdrawing of  $\text{Ni}^{2+}$  complexes.

## Acknowledgement

This work was financially supported by the Postdoctoral Nature Science Foundation of China (No. 080430214).

## References

1. S. C. Tjong and H. Chen: *Mater. Sci. Eng. R*, 2004, **R45**, 1–88.
2. S. J. Askari: *Surf. Eng.*, 2009, **25**, 482–486.
3. X. B. Liang, J. B. Cheng, J. Y. Bai and B. S. Xu: *Surf. Eng.*, 2010, **26**, 209–215.
4. M. Bhardwaj, K. Balani, R. Balasubramaniam, S. Pandey and A. Agarwal: *Surf. Eng.*, 2011, **27**, 642–648.
5. P. Q. Dai, Y. H. Zhong and X. Zhou: *Surf. Eng.*, 2011, **27**, 71–76.
6. C. Z. Zhuo, J. Xu, D. Z. Han and L. L. Liu: *Surf. Eng.*, 2010, **26**, 159–169.
7. S. Dong, B. D. Beake, R. Parkinson and T. Bell: *Surf. Eng.*, 2003, **19**, 195–199.
8. G. Saravanan, S. Mohan, R. M. Gnanamuthu and J. Vijayakumar: *Surf. Eng.*, 2008, **24**, 458–463.
9. J. Xu, J. Tao and S. Y. Jiang: *Mater. Chem. Phys.*, 2008, **112**, 966–972.
10. B. Subramanian, S. Mohan, S. Jayakrishnan and M. Jayachandran: *Curr. Appl. Phys.*, 2007, **7**, 305–313.
11. L. P. Wang, J. Y. Zhang, Y. Gao, Q. J. Xue, L. T. Hu and T. Xu: *Scr. Mater.*, 2006, **55**, 657–660.
12. P. Q. Dai, Z. N. Xiang and W. Z. Chen: *Surf. Eng.*, 2011, **27**, 61–64.
13. R. Mishra, B. Basu and R. Balasubramaniam: *Mater. Sci. Eng. A*, 2004, **A373**, 370–373.
14. X. L. Liu, Z. H. Jiang, Y. W. Guo, Z. H. Zhang and L. Q. Ren: *Thin Solid Films*, 2010, **518**, 3730–3734.
15. J. L. Fang and W. H. Hui (eds.): ‘Brush plating technique’, National Defence Industry Press, Beijing, 1987, 168.
16. P. R. Varadwaj, I. Cukrowski and M. M. Helder: *J. Phys. Chem. A*, 2008, **112**, 10657–10666.
17. R. S. Vemuri, S. K. Gullapalli, D. Zubia, J. C. McClure and C. V. Raman: *Chem. Phys. Lett.*, 2010, **495**, 232–235.
18. E. Rudnik, L. Burzynska, L. Dolasin’ski and M. Misiak: *Appl. Surf. Sci.*, 2010, **256**, 74147420.
19. R. Elansezhian, B. Ramamoorthy and P. Kesavan Nair: *J. Mater. Process. Technol.*, 2009, **209**, 233–240.
20. T. P. Goloub, L. K. Koopal, B. H. Bijsterbosh and M. P. Sidorova: *Langmuir*, 1996, **12**, 3188–3194.
21. M. Alkan, M. Karadaş, M. Doğan and Ö. Demirbaş: *J. Colloid Interf. Sci.*, 2005, **291**, 309–318.